



# Observation of Cabibbo-suppressed and W-exchange $\Lambda_c^+$ baryon decays<sup>1</sup>

The Belle Collaboration

K. Abe<sup>9</sup>, K. Abe<sup>42</sup>, R. Abe<sup>32</sup>, T. Abe<sup>43</sup>, I. Adachi<sup>9</sup>, Byoung Sup Ahn<sup>17</sup>, H. Aihara<sup>44</sup>, M. Akatsu<sup>25</sup>,  
 Y. Asano<sup>49</sup>, T. Aso<sup>48</sup>, V. Aulchenko<sup>2</sup>, T. Aushev<sup>14</sup>, A. M. Bakich<sup>40</sup>, Y. Ban<sup>36</sup>, E. Banas<sup>30</sup>,  
 S. Behari<sup>9</sup>, P. K. Behera<sup>50</sup>, A. Bondar<sup>2</sup>, A. Bozek<sup>30</sup>, T. E. Browder<sup>8</sup>, B. C. K. Casey<sup>8</sup>, P. Chang<sup>29</sup>,  
 Y. Chao<sup>29</sup>, B. G. Cheon<sup>39</sup>, R. Chistov<sup>14</sup>, S.-K. Choi<sup>7</sup>, Y. Choi<sup>39</sup>, L. Y. Dong<sup>12</sup>, A. Drutskoy<sup>14</sup>,  
 S. Eidelman<sup>2</sup>, V. Eiges<sup>14</sup>, Y. Enari<sup>25</sup>, F. Fang<sup>8</sup>, H. Fujii<sup>9</sup>, C. Fukunaga<sup>46</sup>, M. Fukushima<sup>11</sup>,  
 N. Gabyshev<sup>9</sup>, A. Garmash<sup>2,9</sup>, T. Gershon<sup>9</sup>, A. Gordon<sup>23</sup>, R. Guo<sup>27</sup>, J. Haba<sup>9</sup>, H. Hamasaki<sup>9</sup>,  
 F. Handa<sup>43</sup>, K. Hara<sup>34</sup>, T. Hara<sup>34</sup>, N. C. Hastings<sup>23</sup>, H. Hayashii<sup>26</sup>, M. Hazumi<sup>8</sup>, E. M. Heenan<sup>23</sup>,  
 I. Higuchi<sup>43</sup>, T. Higuchi<sup>44</sup>, T. Hojo<sup>34</sup>, T. Hokuue<sup>25</sup>, Y. Hoshi<sup>42</sup>, K. Hoshina<sup>47</sup>, S. R. Hou<sup>29</sup>,  
 W.-S. Hou<sup>29</sup>, S.-C. Hsu<sup>29</sup>, H.-C. Huang<sup>29</sup>, Y. Igarashi<sup>9</sup>, T. Iijima<sup>9</sup>, H. Ikeda<sup>9</sup>, K. Inami<sup>25</sup>,  
 A. Ishikawa<sup>25</sup>, H. Ishino<sup>45</sup>, R. Itoh<sup>9</sup>, H. Iwasaki<sup>9</sup>, Y. Iwasaki<sup>9</sup>, D. J. Jackson<sup>34</sup>, P. Jalocha<sup>30</sup>,  
 H. K. Jang<sup>38</sup>, R. Kagan<sup>14</sup>, J. H. Kang<sup>53</sup>, J. S. Kang<sup>17</sup>, P. Kapusta<sup>30</sup>, N. Katayama<sup>9</sup>, H. Kawai<sup>3</sup>,  
 H. Kawai<sup>44</sup>, N. Kawamura<sup>1</sup>, T. Kawasaki<sup>32</sup>, H. Kichimi<sup>9</sup>, D. W. Kim<sup>39</sup>, Heejong Kim<sup>53</sup>,  
 H. J. Kim<sup>53</sup>, H. O. Kim<sup>39</sup>, Hyunwoo Kim<sup>17</sup>, S. K. Kim<sup>38</sup>, T. H. Kim<sup>53</sup>, K. Kinoshita<sup>5</sup>, H. Konishi<sup>47</sup>,  
 S. Korpar<sup>22,15</sup>, P. Križan<sup>21,15</sup>, P. Krokovny<sup>2</sup>, R. Kulasiri<sup>5</sup>, S. Kumar<sup>35</sup>, A. Kuzmin<sup>2</sup>, Y.-J. Kwon<sup>53</sup>,  
 J. S. Lange<sup>6</sup>, G. Leder<sup>13</sup>, S. H. Lee<sup>38</sup>, D. Liventsev<sup>14</sup>, R.-S. Lu<sup>29</sup>, J. MacNaughton<sup>13</sup>,  
 T. Matsubara<sup>44</sup>, S. Matsumoto<sup>4</sup>, T. Matsumoto<sup>25</sup>, Y. Mikami<sup>43</sup>, K. Miyabayashi<sup>26</sup>, H. Miyake<sup>34</sup>,  
 H. Miyata<sup>32</sup>, G. R. Moloney<sup>23</sup>, S. Mori<sup>49</sup>, T. Mori<sup>4</sup>, T. Nagamine<sup>43</sup>, Y. Nagasaka<sup>10</sup>,  
 Y. Nagashima<sup>34</sup>, T. Nakadaira<sup>44</sup>, E. Nakano<sup>33</sup>, M. Nakao<sup>9</sup>, J. W. Nam<sup>39</sup>, Z. Natkaniec<sup>30</sup>,  
 K. Neichi<sup>42</sup>, S. Nishida<sup>18</sup>, O. Nitoh<sup>47</sup>, S. Noguchi<sup>26</sup>, S. Ogawa<sup>41</sup>, T. Ohshima<sup>25</sup>, T. Okabe<sup>25</sup>,  
 S. Okuno<sup>16</sup>, S. L. Olsen<sup>8</sup>, W. Ostrowicz<sup>30</sup>, H. Ozaki<sup>9</sup>, P. Pakhlov<sup>14</sup>, H. Palka<sup>30</sup>, C. S. Park<sup>38</sup>,  
 C. W. Park<sup>17</sup>, H. Park<sup>19</sup>, K. S. Park<sup>39</sup>, L. S. Peak<sup>40</sup>, J.-P. Perroud<sup>20</sup>, M. Peters<sup>8</sup>, L. E. Piilonen<sup>51</sup>,

<sup>1</sup> submitted to Phys. Lett. B.

M. Satapathy<sup>50</sup>, O. Schneider<sup>20</sup>, S. Schrenk<sup>5</sup>, S. Semenov<sup>14</sup>, K. Senyo<sup>25</sup>, M. E. Sevier<sup>23</sup>,  
H. Shibuya<sup>41</sup>, B. Shwartz<sup>2</sup>, J. B. Singh<sup>35</sup>, S. Stanič<sup>49</sup>, A. Sugi<sup>25</sup>, A. Sugiyama<sup>25</sup>, K. Sumisawa<sup>9</sup>,  
T. Sumiyoshi<sup>9</sup>, K. Suzuki<sup>3</sup>, S. Suzuki<sup>52</sup>, S. Y. Suzuki<sup>9</sup>, S. K. Swain<sup>8</sup>, T. Takahashi<sup>33</sup>, F. Takasaki<sup>9</sup>,  
M. Takita<sup>34</sup>, K. Tamai<sup>9</sup>, N. Tamura<sup>32</sup>, J. Tanaka<sup>44</sup>, M. Tanaka<sup>9</sup>, Y. Tanaka<sup>24</sup>, G. N. Taylor<sup>23</sup>,  
Y. Teramoto<sup>33</sup>, M. Tomoto<sup>9</sup>, T. Tomura<sup>44</sup>, S. N. Tovey<sup>23</sup>, T. Tsuboyama<sup>9</sup>, T. Tsukamoto<sup>9</sup>,  
S. Uehara<sup>9</sup>, K. Ueno<sup>29</sup>, Y. Unno<sup>3</sup>, S. Uno<sup>9</sup>, Y. Ushiroda<sup>9</sup>, S. E. Vahsen<sup>37</sup>, K. E. Varvell<sup>40</sup>,  
C. C. Wang<sup>29</sup>, C. H. Wang<sup>28</sup>, J. G. Wang<sup>51</sup>, M.-Z. Wang<sup>29</sup>, Y. Watanabe<sup>45</sup>, E. Won<sup>38</sup>,  
B. D. Yabsley<sup>9</sup>, Y. Yamada<sup>9</sup>, M. Yamaga<sup>43</sup>, A. Yamaguchi<sup>43</sup>, Y. Yamashita<sup>31</sup>, M. Yamauchi<sup>9</sup>,  
S. Yanaka<sup>45</sup>, J. Yashima<sup>9</sup>, M. Yokoyama<sup>44</sup>, K. Yoshida<sup>25</sup>, Y. Yuan<sup>12</sup>, Y. Yusa<sup>43</sup>, C. C. Zhang<sup>12</sup>,  
J. Zhang<sup>49</sup>, H. W. Zhao<sup>9</sup>, Y. Zheng<sup>8</sup>, V. Zhilich<sup>2</sup>, and D. Žontar<sup>49</sup>

<sup>1</sup>Aomori University, Aomori

<sup>2</sup>Budker Institute of Nuclear Physics, Novosibirsk

<sup>3</sup>Chiba University, Chiba

<sup>4</sup>Chuo University, Tokyo

<sup>5</sup>University of Cincinnati, Cincinnati OH

<sup>6</sup>University of Frankfurt, Frankfurt

<sup>7</sup>Gyeongsang National University, Chinju

<sup>8</sup>University of Hawaii, Honolulu HI

<sup>9</sup>High Energy Accelerator Research Organization (KEK), Tsukuba

<sup>10</sup>Hiroshima Institute of Technology, Hiroshima

<sup>11</sup>Institute for Cosmic Ray Research, University of Tokyo, Tokyo

<sup>12</sup>Institute of High Energy Physics, Chinese Academy of Sciences, Beijing

<sup>13</sup>Institute of High Energy Physics, Vienna

<sup>14</sup>Institute for Theoretical and Experimental Physics, Moscow

<sup>15</sup>J. Stefan Institute, Ljubljana

<sup>16</sup>Kanagawa University, Yokohama

<sup>17</sup>Korea University, Seoul

<sup>18</sup>Kyoto University, Kyoto

<sup>19</sup>Kyungpook National University, Taegu

<sup>20</sup>IPHE, University of Lausanne, Lausanne

<sup>21</sup>University of Ljubljana, Ljubljana

<sup>22</sup>University of Maribor, Maribor

<sup>23</sup>University of Melbourne, Victoria

<sup>24</sup>Nagasaki Institute of Applied Science, Nagasaki

<sup>25</sup>Nagoya University, Nagoya

<sup>26</sup>Nara Women's University, Nara

<sup>27</sup>National Kaohsiung Normal University, Kaohsiung

<sup>28</sup>National Lien-Ho Institute of Technology, Miao Li

<sup>29</sup>National Taiwan University, Taipei

<sup>30</sup>H. Niewodniczanski Institute of Nuclear Physics, Krakow

- <sup>32</sup>Niigata University, Niigata  
<sup>33</sup>Osaka City University, Osaka  
<sup>34</sup>Osaka University, Osaka  
<sup>35</sup>Panjab University, Chandigarh  
<sup>36</sup>Peking University, Beijing  
<sup>37</sup>Princeton University, Princeton NJ  
<sup>38</sup>Seoul National University, Seoul  
<sup>39</sup>Sungkyunkwan University, Suwon  
<sup>40</sup>University of Sydney, Sydney NSW  
<sup>41</sup>Toho University, Funabashi  
<sup>42</sup>Tohoku Gakuin University, Tagajo  
<sup>43</sup>Tohoku University, Sendai  
<sup>44</sup>University of Tokyo, Tokyo  
<sup>45</sup>Tokyo Institute of Technology, Tokyo  
<sup>46</sup>Tokyo Metropolitan University, Tokyo  
<sup>47</sup>Tokyo University of Agriculture and Technology, Tokyo  
<sup>48</sup>Toyama National College of Maritime Technology, Toyama  
<sup>49</sup>University of Tsukuba, Tsukuba  
<sup>50</sup>Utkal University, Bhubaneswer  
<sup>51</sup>Virginia Polytechnic Institute and State University, Blacksburg VA  
<sup>52</sup>Yokkaichi University, Yokkaichi  
<sup>53</sup>Yonsei University, Seoul

We present measurements of the Cabibbo-suppressed decays  $\Lambda_c^+ \rightarrow \Lambda^0 K^+$  and  $\Lambda_c^+ \rightarrow \Sigma^0 K^+$  (both first observations),  $\Lambda_c^+ \rightarrow \Sigma^+ K^+ \pi^-$  (seen with large statistics for the first time),  $\Lambda_c^+ \rightarrow p K^+ K^-$  and  $\Lambda_c^+ \rightarrow p \phi$  (measured with improved accuracy). Improved branching ratio measurements for the decays  $\Lambda_c^+ \rightarrow \Sigma^+ K^+ K^-$  and  $\Lambda_c^+ \rightarrow \Sigma^+ \phi$ , which are attributed to W-exchange diagrams, are shown. We also present the first evidence for  $\Lambda_c^+ \rightarrow \Xi(1690)^0 K^+$  and set an upper limit on the non-resonant decay  $\Lambda_c^+ \rightarrow \Sigma^+ K^+ K^-$ . This analysis was performed using  $32.6 \text{ fb}^{-1}$  of data collected by the Belle detector at the asymmetric  $e^+e^-$  collider KEKB.

## 1 Introduction

Decays of charmed baryons, unlike charmed mesons, are not colour or helicity suppressed, allowing us to investigate the contribution of W-exchange diagrams. There are also possible interference effects due to the presence of identical quarks. This makes the study of these decays a useful tool to test theoretical models that predict exclusive decay rates [1].

During the past several years there has been significant progress in the experimental study of hadronic decays of charmed baryons. New results on masses, widths, lifetimes and decay asymmetry parameters have been published by various experiments [2]. However the accuracy of branching ratio measurements does not exceed 30% for many Cabibbo-favoured modes: for Cabibbo-suppressed and W-exchange dominated decays, the experimental accuracy is even worse. As a result, we are not yet able to conclusively distinguish between the decay rate predictions made by different theoretical models.

In this paper we present a study of  $\Lambda_c^+$  baryons produced in the  $e^+e^- \rightarrow q\bar{q}$  continuum at Belle, relying on the excellent particle identification capability of the detector to measure decays with kaons in the final state. We report the first observation of the Cabibbo-suppressed decays  $\Lambda_c^+ \rightarrow \Lambda^0 K^+$  and  $\Lambda_c^+ \rightarrow \Sigma^0 K^+$ , and the first observation of  $\Lambda_c^+ \rightarrow \Sigma^+ K^+ \pi^-$  with large statistics. (Here and throughout this paper, the inclusion of charge-conjugate states is implied.) We present improved measurements of the Cabibbo-suppressed decays  $\Lambda_c^+ \rightarrow p K^+ K^-$  and  $\Lambda_c^+ \rightarrow p \phi$ , and the W-exchange decays  $\Lambda_c^+ \rightarrow \Sigma^+ K^+ K^-$  and  $\Lambda_c^+ \rightarrow \Sigma^+ \phi$ ; we also report the first evidence for  $\Lambda_c^+ \rightarrow \Xi(1690)^0 K^+$ , and set an upper limit on non-resonant  $\Lambda_c^+ \rightarrow \Sigma^+ K^+ K^-$  decay.

## 2 Data and Selection Criteria

The data used for this analysis were taken on the  $\Upsilon(4S)$  resonance and in the nearby continuum using the Belle detector at the asymmetric  $e^+e^-$  collider KEKB. The integrated luminosity of the data sample is equal to  $32.6 \text{ fb}^{-1}$ .

Belle is a general purpose detector based on a 1.5 T superconducting solenoid; a detailed description can be found elsewhere [3]. Tracking is performed with a silicon vertex detector (SVD) composed of three concentric layers of double-sided silicon strip detectors, and a 50 layer drift chamber. Particle identification for charged hadrons, important for the measurement of final states with

chamber, time of flight measurements and aerogel Cerenkov counter information. For each charged track, measurements from these three subdetectors are combined to form  $K/\pi$  and  $p/K$  likelihood ratios in the range from 0 to 1,

$$P(K/\pi) = \mathcal{L}(K)/(\mathcal{L}(K) + \mathcal{L}(\pi)), \quad P(p/K) = \mathcal{L}(p)/(\mathcal{L}(p) + \mathcal{L}(K)),$$

where  $\mathcal{L}(p)$ ,  $\mathcal{L}(K)$  and  $\mathcal{L}(\pi)$  are the likelihood values assigned to each identification hypothesis for a given track.

For the analyses presented here, we require  $P(K/\pi) < 0.9$  for pions,  $P(K/\pi) > 0.6$  for kaons, and  $P(p/K) > 0.9$  for protons, unless stated otherwise. Candidate  $\pi^0$ 's are reconstructed from pairs of photons detected in the CsI calorimeter, with a minimum energy of 50 MeV per photon. The interaction point (IP) coordinates in the  $r-\phi$  plane are determined from beam profile measurements. Other particles are identified as follows:

- $\Lambda^0$  are reconstructed in the decay mode  $\Lambda^0 \rightarrow p\pi^-$ , fitting the  $p$  and  $\pi^-$  tracks to a common vertex and requiring an invariant mass in a  $\pm 3 \text{ MeV}/c^2$  ( $\approx \pm 3\sigma$ ) interval around the nominal value. The likelihood ratio cut on the proton is relaxed to  $P(p/K) > 0.4$ . We then make the following cuts on the  $\Lambda^0$  decay vertex:
  - the closest distance of approach along the beam direction between the proton and pion tracks must be less than 1 cm;
  - the distance between the decay vertex and the interaction point in the  $r-\phi$  plane must be greater than 1 mm;
  - the cosine of the angle in the  $r-\phi$  plane between the  $\Lambda^0$  momentum vector and the vector pointing from the IP to the decay vertex must be greater than 0.995.
- $K_S^0$  are reconstructed in the decay mode  $K_S^0 \rightarrow \pi^+\pi^-$ , fitting the  $\pi^+$  and  $\pi^-$  tracks to a common vertex and requiring an invariant mass in a  $\pm 7 \text{ MeV}/c^2$  ( $\approx \pm 3\sigma$ ) interval around the nominal value. We then make the same vertex cuts as in the  $\Lambda^0$  case.
- $\Sigma^+$  are reconstructed in the decay mode  $\Sigma^+ \rightarrow p\pi^0$ , requiring an invariant mass within  $\pm 10 \text{ MeV}/c^2$  ( $\approx \pm 2\sigma$ ) of the nominal value. We require the proton to have at least one hit in the SVD, to improve its impact parameter resolution with respect to the IP; we then require the impact parameter in the  $r-\phi$  plane to be greater than  $200 \mu\text{m}$ , to make sure the  $\Sigma^+$  vertex is displaced from the IP.
- $\Sigma^0 \rightarrow \Lambda^0\gamma$  decays are formed using identified  $\Lambda^0$  and photons with calorimeter cluster energies above 0.1 GeV; we accept candidates with invariant masses within  $\pm 6 \text{ MeV}/c^2$  ( $\approx \pm 1.5\sigma$ ) of the nominal value.

To suppress combinatorial and  $B\bar{B}$  backgrounds, we require  $\Lambda_c^+$  candidates to have scaled momentum  $x_p = p^*/p_{\text{max}}^* > 0.5$ ; here  $p^*$  is the reconstructed momentum of the  $\Lambda_c^+$  candidate in the

the reconstructed mass of the  $\Lambda_c^+$  candidate. In modes where there are two or more charged tracks at the  $\Lambda_c^+$  vertex, we perform a vertex fit and require  $\chi^2/\text{n.d.f.} < 9$ .

In the various mass fits described below, the central value and width of the signal peaks are always allowed to float, unless stated otherwise. Wherever the final state includes a hyperon, we improve the invariant mass resolution by plotting the corrected mass difference, *e.g.*  $M(\Sigma^+ K^+ K^-) - M(\Sigma^+) + M_{\Sigma^+}^{\text{PDG}}$  instead of  $M(\Sigma^+ K^+ K^-)$ .

### 3 Observation of the decays $\Lambda_c^+ \rightarrow \Lambda^0 K^+$ and $\Lambda_c^+ \rightarrow \Sigma^0 K^+$

The Cabibbo-suppressed decay  $\Lambda_c^+ \rightarrow \Lambda^0 K^+$  has not been previously observed. Reconstructing  $\Lambda^0 K^+$  combinations as described in Section 2, we see a clear signal at the  $\Lambda_c^+$  mass, as shown in Fig. 1.

To study backgrounds due to Cabibbo-allowed decays, we select a second sample with a reversed identification requirement  $P(K/\pi) < 0.1$  applied to the “kaon”. In the mass spectrum of this sample, where the kaon mass hypothesis is still used, we see a broad structure centered around  $2.4 \text{ GeV}/c^2$ , produced by  $\Lambda_c^+ \rightarrow \Lambda^0 \pi^+$  and  $\Lambda_c^+ \rightarrow \Sigma^0 \pi^+$  decays. We fit this distribution using two Gaussians (to

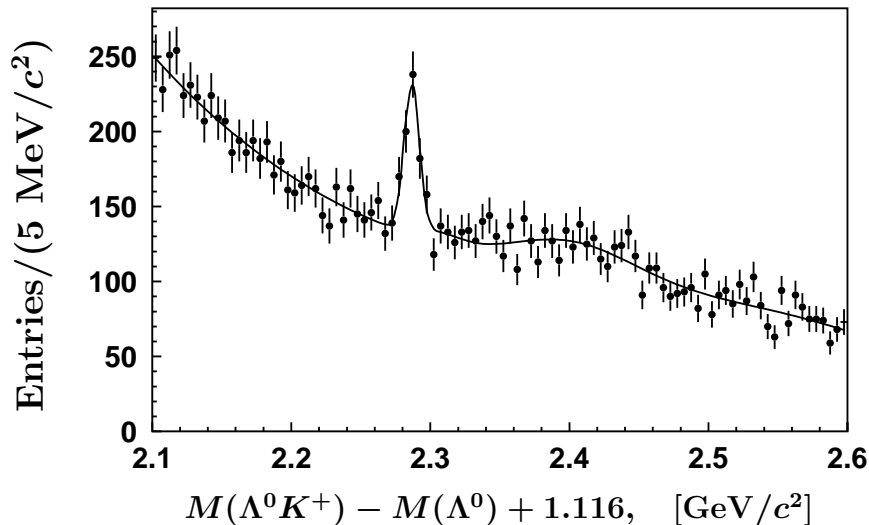


Figure 1:  $\Lambda_c^+ \rightarrow \Lambda^0 K^+$ : invariant mass spectrum of the selected  $\Lambda^0 K^+$  combinations. The broad structure to the right of the signal peak, due to  $\Lambda_c^+ \rightarrow \Lambda^0 \pi^+$  and  $\Lambda_c^+ \rightarrow \Sigma^0 \pi^+$  decays, is included in the fit.

model the  $\Lambda_c^+ \rightarrow \Lambda^0 \pi^+$  and  $\Lambda_c^+ \rightarrow \Sigma^0 \pi^+$  contributions), and a second order polynomial (to model the broad reflections and the remaining background). The shape of this function is then used to model the  $\Lambda_c^+ \rightarrow \Lambda^0 \pi^+(\Sigma^0 \pi^+)$  background in the main sample. The remaining combinatorial background in Fig. 1 is represented using a second order polynomial, and the  $\Lambda_c^+ \rightarrow \Lambda^0 K^+$  signal is described by a Gaussian with width  $\sigma = 5.4 \text{ MeV}/c^2$  (fixed from Monte Carlo); the result of the fit is shown by the superimposed curve. We find a yield of  $265 \pm 35$   $\Lambda_c^+ \rightarrow \Lambda^0 K^+$  decays, the first observation of this decay mode.

with a Gaussian for the signal and a second order polynomial for the background. We find  $4550 \pm 111$  events. The relative reconstruction efficiency was determined using, Monte Carlo simulation (MC), to be  $\epsilon(\Lambda_c^+ \rightarrow \Lambda^0 K^+)/\epsilon(\Lambda_c^+ \rightarrow \Lambda^0 \pi^+) = 0.79$ . Using this value, we extract

$$\frac{\mathcal{B}(\Lambda_c^+ \rightarrow \Lambda^0 K^+)}{\mathcal{B}(\Lambda_c^+ \rightarrow \Lambda^0 \pi^+)} = 0.074 \pm 0.010 \pm 0.012;$$

the first error is statistical, and the second is systematic. We provide a detailed description of the sources of systematic error for this and other measured decay modes in Section 8.

The Cabibbo-suppressed decay  $\Lambda_c^+ \rightarrow \Sigma^0 K^+$  is reconstructed in a similar way, with the scaled momentum cut tightened to  $x_p > 0.6$  to suppress the large background due to soft photons. The invariant mass distribution of the selected  $\Sigma^0 K^+$  candidates is shown in Fig. 2: a peak is seen at the  $\Lambda_c^+$  mass, and a reflection due to misidentified two-body Cabibbo-allowed  $\Lambda_c^+$  decays is seen at higher masses. The superimposed curve shows the result of a fit following the method described for  $\Lambda^0 K^+$ , with the exception that in this case the width of the signal Gaussian is fixed from the MC to  $\sigma = 5.0 \text{ MeV}/c^2$ . We find  $75 \pm 18$   $\Lambda_c^+ \rightarrow \Sigma^0 K^+$  events, the first observation of this decay mode. For normalization, we use the decay  $\Lambda_c^+ \rightarrow \Sigma^0 \pi^+$ . We fit the distribution with a Gaussian for the signal,

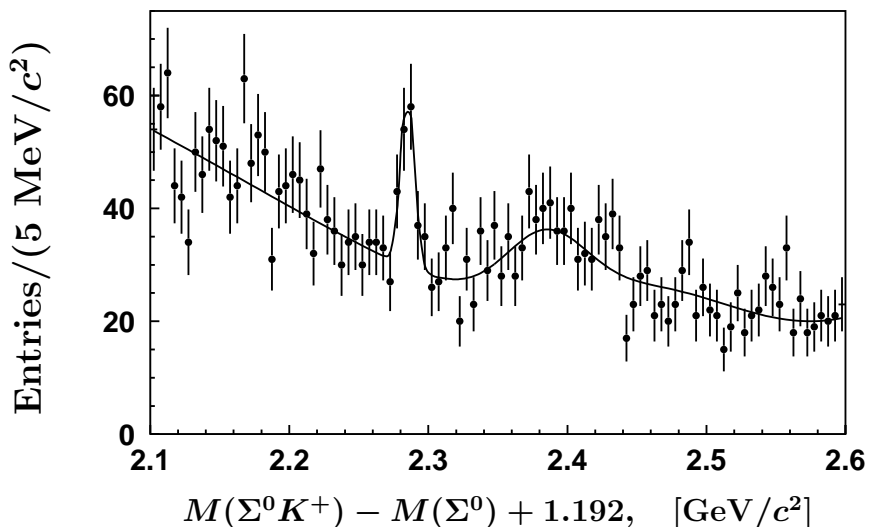


Figure 2:  $\Lambda_c^+ \rightarrow \Sigma^0 K^+$ : invariant mass spectrum of the selected  $\Sigma^0 K^+$  combinations. The broad structure to the right of the signal peak, due to  $\Lambda_c^+ \rightarrow \Lambda^0 \pi^+$  and  $\Lambda_c^+ \rightarrow \Sigma^0 \pi^+$  decays, is included in the fit.

a second Gaussian to describe the broad enhancement due to  $\Lambda_c^+ \rightarrow \Lambda^0 \pi^+$  (with the addition of a random  $\gamma$ ), and a second order polynomial for the remaining background. The fit gives  $1597 \pm 67$   $\Lambda_c^+ \rightarrow \Sigma^0 \pi^+$  decays. The relative reconstruction efficiency found to be  $\epsilon(\Lambda_c^+ \rightarrow \Sigma^0 K^+)/\epsilon(\Lambda_c^+ \rightarrow \Sigma^0 \pi^+) = 0.84$  in the MC: we then calculate

$$\frac{\mathcal{B}(\Lambda_c^+ \rightarrow \Sigma^0 K^+)}{\mathcal{B}(\Lambda_c^+ \rightarrow \Sigma^0 \pi^+)} = 0.056 \pm 0.014 \pm 0.008.$$

The first evidence for the Cabibbo-suppressed decay  $\Lambda_c^+ \rightarrow \Sigma^+ K^+ \pi^-$  was published by the NA32 collaboration in 1992 [4]: they found 2 events in the signal region. Reconstructing  $\Sigma^+ K^+ \pi^-$  combinations with the cuts of Section 2 tightened to require  $x_p > 0.6$ , we see a clear signal peak at the  $\Lambda_c^+$  mass, as shown in Fig. 3. The tighter cut is used to suppress the large combinatorial background. We also form  $\Sigma^+ K^+ \pi^-$  combinations using “ $\Sigma^+$ ” candidates from mass sidebands (two 10  $\text{MeV}/c^2$  intervals centered 20  $\text{MeV}/c^2$  below and above the nominal  $\Sigma^+$  mass [2]), shown with the shaded histogram: no enhancement is seen near the  $\Lambda_c^+$  mass.

The mass distribution is fitted with a Gaussian for the signal (with width fixed to 3.6  $\text{MeV}/c^2$  from the MC) and a second order polynomial for the background: we find  $105 \pm 24$   $\Lambda_c^+ \rightarrow \Sigma^+ K^+ \pi^-$  events. For normalization we reconstruct  $\Lambda_c^+ \rightarrow \Sigma^+ \pi^+ \pi^-$  decays with the same cuts, finding  $2368 \pm 89$  events. The relative efficiency of the  $\Lambda_c^+ \rightarrow \Sigma^+ K^+ \pi^-$  channel reconstruction with respect to  $\Lambda_c^+ \rightarrow \Sigma^+ \pi^+ \pi^-$  is found to be 0.94 in the MC. Using this value, we obtain

$$\frac{\mathcal{B}(\Lambda_c^+ \rightarrow \Sigma^+ K^+ \pi^-)}{\mathcal{B}(\Lambda_c^+ \rightarrow \Sigma^+ \pi^+ \pi^-)} = 0.047 \pm 0.011 \pm 0.008.$$

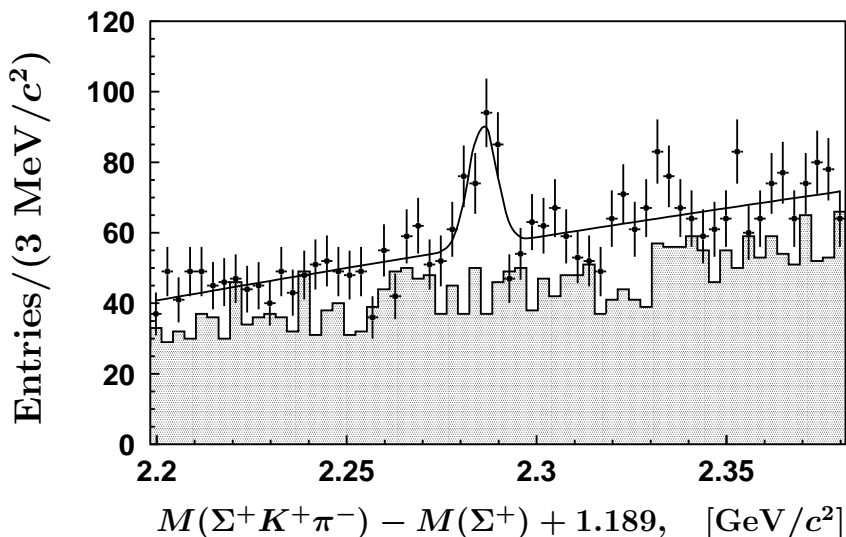


Figure 3:  $\Lambda_c^+ \rightarrow \Sigma^+ K^+ \pi^-$ : invariant mass spectrum of the selected  $\Sigma^+ K^+ \pi^-$  combinations. The shaded histogram shows the equivalent spectrum for the  $\Sigma^+$  sidebands. The mass difference for the sidebands is corrected using the central value of the corresponding sideband interval.

## 5 Measurement of the $\Lambda_c^+ \rightarrow \Sigma^+ K^+ K^-$ and $\Sigma^+ \phi$ decays

The decays  $\Lambda_c^+ \rightarrow \Sigma^+ K^+ K^-$  and  $\Lambda_c^+ \rightarrow \Sigma^+ \phi$  proceed dominantly via W-exchange diagrams, and were observed by CLEO in 1993 [5]. Here we measure these decay channels with improved accuracy and provide the first evidence for the  $\Lambda_c^+ \rightarrow \Xi(1690)^0 K^+$  decay.



to Section 2. A clear peak is seen at the  $\Lambda_c^+$  mass, over a low background. We fit the distribution using

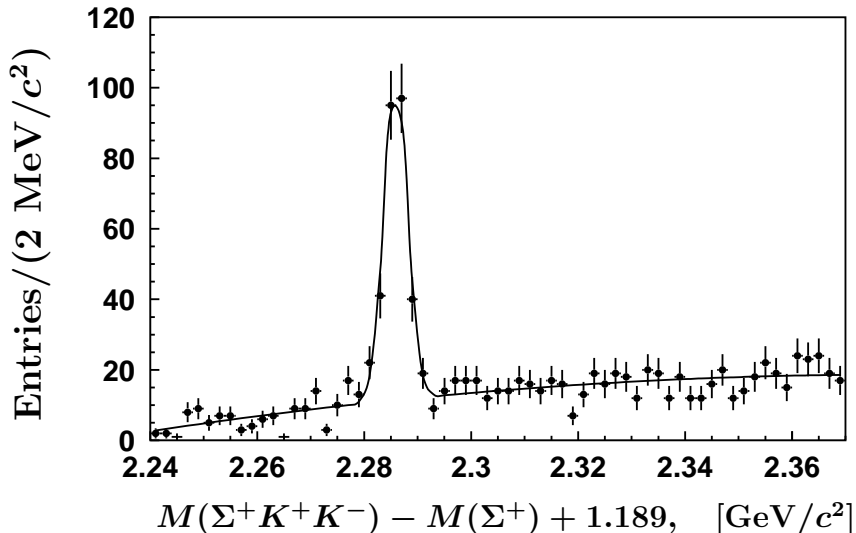


Figure 4:  $\Lambda_c^+ \rightarrow \Sigma^+ K^+ K^-$ : invariant mass spectrum of the selected  $\Sigma^+ K^+ K^-$  combinations.

a Gaussian (with width fixed to  $2.2 \text{ MeV}/c^2$  from the MC) plus a second order polynomial: the fit yields  $246 \pm 20$   $\Lambda_c^+ \rightarrow \Sigma^+ K^+ K^-$  decays. For normalization we reconstruct the  $\Lambda_c^+ \rightarrow \Sigma^+ \pi^+ \pi^-$  decay mode with equivalent cuts, and fit the distribution with a Gaussian and a second order polynomial: we find  $3650 \pm 138$   $\Lambda_c^+ \rightarrow \Sigma^+ \pi^+ \pi^-$  events. The relative efficiency of the  $\Lambda_c^+ \rightarrow \Sigma^+ K^+ K^-$  decay reconstruction with respect to the  $\Lambda_c^+ \rightarrow \Sigma^+ \pi^+ \pi^-$  decay is calculated by MC simulation and is found to be 0.89. We thus extract

$$\frac{\mathcal{B}(\Lambda_c^+ \rightarrow \Sigma^+ K^+ K^-)}{\mathcal{B}(\Lambda_c^+ \rightarrow \Sigma^+ \pi^+ \pi^-)} = 0.076 \pm 0.007 \pm 0.009.$$

In order to obtain the  $\Lambda_c^+ \rightarrow \Sigma^+ \phi$  signal, we take  $\Sigma^+ K^+ K^-$  from a  $\pm 5 \text{ MeV}/c^2$  window around the fitted  $\Lambda_c^+$  mass ( $2286 \text{ MeV}/c^2$ ), and plot the invariant mass of the  $K^+ K^-$  combination, as shown in Fig. 5 (points with error bars); the equivalent distribution is also shown for  $\Sigma^+ K^+ K^-$  in  $5 \text{ MeV}/c^2$  sidebands centered  $12.5 \text{ MeV}/c^2$  below and above the fitted  $\Lambda_c^+$  mass (shaded histogram). The distributions are fitted with a Breit-Wigner function (describing the  $\phi$  signal) convolved with a Gaussian of fixed width (representing the detector mass resolution) plus a second order polynomial multiplied by a square root threshold factor. The intrinsic width of the  $\phi$  Breit-Wigner function is fixed to its nominal value [2], and the width of the Gaussian resolution is fixed to  $1.0 \text{ MeV}/c^2$  based on the MC simulation. The fit yields  $153 \pm 15$  events for the  $\phi$  signal in the  $\Lambda_c^+$  region and  $27 \pm 7$  in the  $\Lambda_c^+$  sidebands. To extract the  $\Lambda_c^+ \rightarrow \Sigma^+ \phi$  contribution we subtract the  $\phi$  yield in the sidebands from the yield in the  $\Lambda_c^+$  signal region, correcting for the phase space factor obtained from the  $\Sigma^+ K^+ K^-$  background fitting function. After making a further correction for the missing signal outside the  $\Lambda_c^+$  mass interval, we obtain  $129 \pm 17$   $\Lambda_c^+ \rightarrow \Sigma^+ \phi$  decays.

The relative efficiency of the  $\Lambda_c^+ \rightarrow \Sigma^+ \phi$  reconstruction with respect to  $\Lambda_c^+ \rightarrow \Sigma^+ \pi^+ \pi^-$  is calculated using the MC and found to be 0.84. Taking into account the  $\phi$  branching fraction

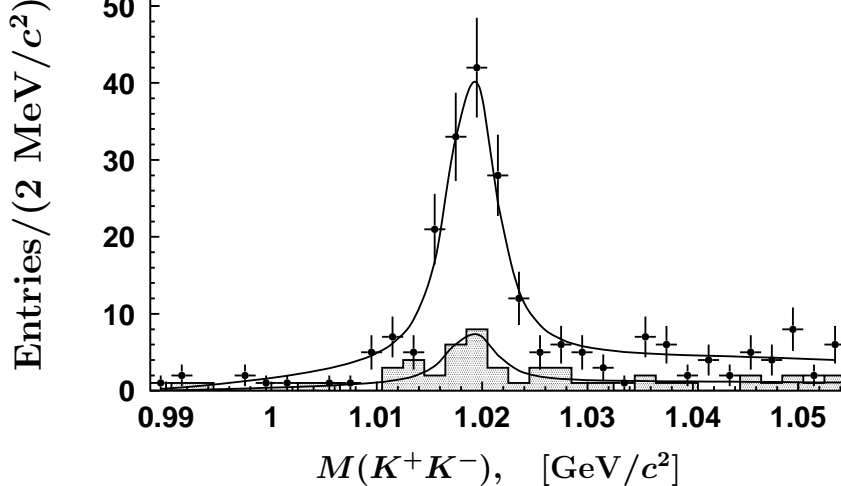


Figure 5: Fitting for the  $\Lambda_c^+ \rightarrow \Sigma^+ \phi$  component: the invariant mass spectra of  $K^+ K^-$  combinations from the  $\Lambda_c^+ \rightarrow \Sigma^+ K^+ K^-$  signal area (points with error bars) and  $\Lambda_c^+$  sidebands (shaded histogram) are shown.

$\mathcal{B}(\phi \rightarrow K^+ K^-) = (49.4 \pm 0.7)\%$  [2], we calculate

$$\frac{\mathcal{B}(\Lambda_c^+ \rightarrow \Sigma^+ \phi)}{\mathcal{B}(\Lambda_c^+ \rightarrow \Sigma^+ \pi^+ \pi^-)} = 0.085 \pm 0.012 \pm 0.012.$$

We also search for resonant structure in the  $\Sigma^+ K^-$  system in these decays. Figure 6 shows the  $\Sigma^+ K^-$  invariant mass spectrum for  $\Sigma^+ K^+ K^-$  combinations in a  $\pm 5 \text{ MeV}/c^2$  interval around the fitted  $\Lambda_c^+$  mass (data points): we also require  $|M(K^+ K^-) - m_\phi| > 10 \text{ MeV}/c^2$  to suppress  $\phi \rightarrow K^+ K^-$ . Also shown is the  $\Sigma^+ K^-$  invariant mass spectrum from  $\Sigma^+ K^+ K^-$  combinations selected inside  $5 \text{ MeV}/c^2$  sideband intervals centered  $12.5 \text{ MeV}/c^2$  below and above the fitted  $\Lambda_c^+$  mass (shaded histogram). The  $\Sigma^+ K^-$  mass distribution shows evidence for the  $\Xi(1690)^0$  resonant state. In order to extract this resonant contribution the histograms are fitted with a relativistic Breit-Wigner function (describing the  $\Xi(1690)^0$  signal) plus a  $(M_{\text{max}} - M)^\alpha$  function multiplied by a square root threshold factor (here  $M_{\text{max}}$  is the maximal allowed value of the  $\Sigma^+ K^-$  invariant mass). The fit yields  $82 \pm 15$  events for the  $\Xi(1690)^0$  signal in the  $\Lambda_c^+$  region, with a fitted mass  $(1688 \pm 2) \text{ MeV}/c^2$  and width  $(11 \pm 4) \text{ MeV}$  in good agreement with previous measurements of the  $\Xi(1690)^0$  parameters [2]. To fit the sidebands, the function parameters are fixed to the central values obtained from the signal fit, and both the signal and background normalizations are floated. A yield of  $9 \pm 4$  events is found.

The  $\Lambda_c^+ \rightarrow \Xi(1690)^0 K^+$  contribution is obtained by subtracting the  $\Xi(1690)^0$  yield in the sidebands from the yield in the  $\Lambda_c^+$  signal region, correcting the sideband contribution using the phase space factor obtained from the  $\Sigma^+ K^+ K^-$  background fitting function. After a further correction for the missing signal outside the  $\Lambda_c^+$  mass interval, we obtain  $75 \pm 16$   $\Lambda_c^+ \rightarrow \Xi(1690)^0 K^+$  decays. We then find

$$\frac{\mathcal{B}(\Lambda_c^+ \rightarrow \Xi(1690)^0 K^+)}{\mathcal{B}(\Lambda_c^+ \rightarrow \Sigma^+ \pi^+ \pi^-)} \times \mathcal{B}(\Xi(1690)^0 \rightarrow \Sigma^+ K^-) = 0.023 \pm 0.005 \pm 0.005;$$

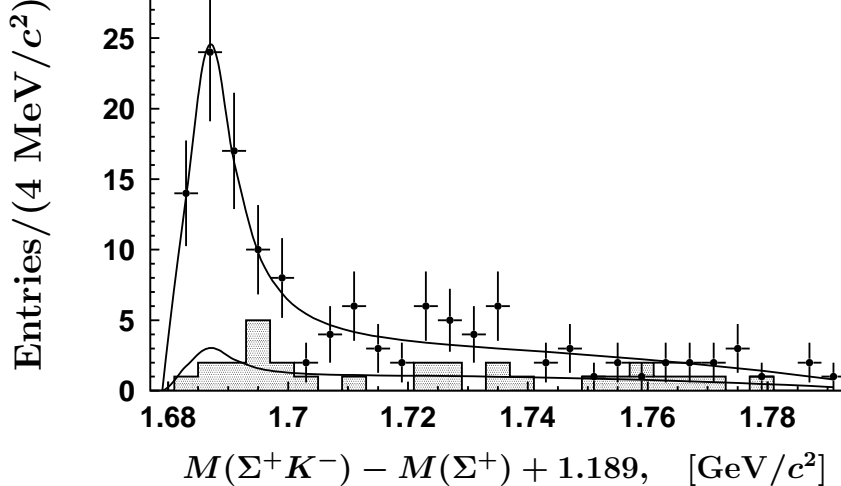


Figure 6: Fitting for the  $\Lambda_c^+ \rightarrow \Xi(1690)^0 K^+$  component: the invariant mass spectrum of  $\Sigma^+ K^-$  combinations from the  $\Lambda_c^+ \rightarrow \Sigma^+ K^+ K^-$  signal area (points with error bars) and  $\Lambda_c^+$  sidebands (shaded histogram) are shown, with the  $\phi \rightarrow K^+ K^-$  signal region excluded in both cases.

the possible effects due to interference with  $\Lambda_c^+ \rightarrow \Sigma^+ \phi$  are included in the systematic error (see the discussion in Section 8).

Finally, the non-resonant  $\Lambda_c^+ \rightarrow \Sigma^+ K^+ K^-$  contribution is estimated by making invariant mass cuts  $|M(K^+ K^-) - m_\phi| > 10 \text{ MeV}/c^2$  and  $|M(\Sigma^+ K^-) - M_{\Xi(1690)^0}| > 20 \text{ MeV}/c^2$  to suppress the  $\phi$  and  $\Xi(1690)^0$  contributions (here,  $M_{\Xi(1690)^0}$  is the fitted  $\Xi(1690)^0$  mass). The resulting  $\Sigma^+ K^+ K^-$  mass spectrum is fitted with a Gaussian (with width fixed to  $2.2 \text{ MeV}/c^2$  from the MC) plus a second order polynomial. The fit yields  $34 \pm 9$  events. Integrating the  $\phi$  Breit-Wigner function over the allowed  $M(K^+ K^-)$  region, we find that 14% of the total  $\Lambda_c^+ \rightarrow \Sigma^+ \phi$  signal contributes to this sample:  $18 \pm 3$  events. The contribution of the  $\Xi(1690)^0$  mass tails is estimated to be approximately 12% of the fitted  $\Xi(1690)^0$  signal:  $9 \pm 2$  events. Subtracting these contributions,  $7 \pm 10$  non-resonant events remain. The phase space correction factor to account for the missing region around the  $\phi$  and  $\Xi(1690)^0$  masses is found to be 1.63 by MC simulation of the non-resonant  $M(K^+ K^-)$  spectrum. Applying this correction we obtain  $11 \pm 16$   $\Lambda_c^+ \rightarrow \Sigma^+ K^+ K^-$  non-resonant decays. Taking into account the systematic error, we obtain an upper limit

$$\frac{\mathcal{B}(\Lambda_c^+ \rightarrow \Sigma^+ K^+ K^-)_{\text{non-res}}}{\mathcal{B}(\Lambda_c^+ \rightarrow \Sigma^+ \pi^+ \pi^-)} < 0.018$$

at the 90% confidence level, including the possible effects due to interference with  $\Lambda_c^+ \rightarrow \Sigma^+ \phi$  in the systematic errors (see Section 8).

## 6 Evidence for the $\Xi(1690)^0$ in $\Lambda_c^+ \rightarrow \Lambda^0 \bar{K}^0 K^+$ decays

Another possible decay mode of the  $\Xi(1690)^0$  resonant state is  $\Xi(1690)^0 \rightarrow \Lambda^0 \bar{K}^0$ . Hence we have searched for the decay  $\Lambda_c^+ \rightarrow \Xi(1690)^0 K^+$  by reconstructing  $\Lambda_c^+ \rightarrow \Lambda^0 K_S^0 K^+$  decays and looking

Section 2 we obtain an invariant mass spectrum, which is fitted with a Gaussian for the signal and a second order polynomial for the background: we find  $363 \pm 26 \Lambda_c^+ \rightarrow \Lambda^0 K_S^0 K^+$  events. In order to obtain the  $\Lambda_c^+ \rightarrow \Xi(1690)^0 K^+$  signal, we take  $\Lambda^0 K_S^0 K^+$  from a  $\pm 10 \text{ MeV}/c^2$  window ( $\approx 2.5\sigma$ ) around the fitted  $\Lambda_c^+$  mass ( $2287 \text{ MeV}/c^2$ ), and plot the invariant mass of the  $\Lambda^0 K_S^0$  combination, as shown in Fig. 7 (points with error bars); the equivalent distribution is also shown for  $\Lambda^0 K_S^0 K^+$  from  $10 \text{ MeV}/c^2$  sideband intervals centered  $20 \text{ MeV}/c^2$  below and above the fitted  $\Lambda_c^+$  mass (shaded histogram). A peak at the expected position is clearly seen. We use a fitting procedure similar to that described in

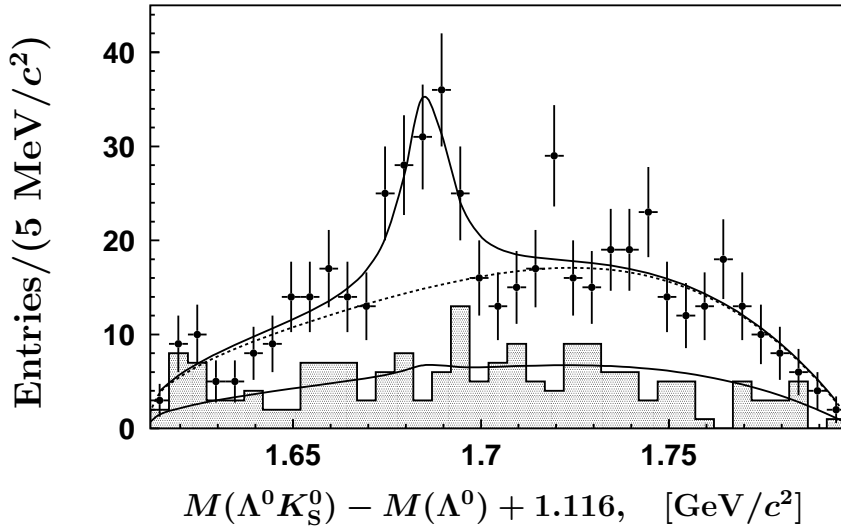


Figure 7: Fitting for the  $\Lambda_c^+ \rightarrow \Xi(1690)^0 K^+$  component: the invariant mass spectrum of  $\Lambda^0 K_S^0$  combinations from the  $\Lambda_c^+ \rightarrow \Lambda^0 K_S^0 K^+$  signal area (points with error bars) and  $\Lambda_c^+$  sidebands (shaded histogram) are shown. The dashed curve represents the background function.

Section 5 for the  $\Lambda_c^+ \rightarrow \Sigma^+ \phi$  analysis. After subtraction of the sideband contribution and corrections we obtain  $93 \pm 26 \Lambda_c^+ \rightarrow \Xi(1690)^0 K^+$  decays. This confirms our observation of the  $\Lambda_c^+ \rightarrow \Xi(1690)^0 K^+$  decay: significant signals are seen for both  $\Xi(1690)^0 \rightarrow \Sigma^+ K^-$  and  $\Xi(1690)^0 \rightarrow \Lambda^0 \bar{K}^0$ .

Using the normalization to the inclusive decay mode  $\Lambda_c^+ \rightarrow \Lambda^0 \bar{K}^0 K^+$  and the measured values for the  $\mathcal{B}(\Lambda_c^+ \rightarrow \Sigma^+ \pi^+ \pi^-)$  and  $\mathcal{B}(\Lambda_c^+ \rightarrow \Lambda^0 \bar{K}^0 K^+)$  [2] we find

$$\frac{\mathcal{B}(\Lambda_c^+ \rightarrow \Xi(1690)^0 K^+)}{\mathcal{B}(\Lambda_c^+ \rightarrow \Lambda^0 \bar{K}^0 K^+)} \times \mathcal{B}(\Xi(1690)^0 \rightarrow \Lambda^0 \bar{K}^0) = 0.26 \pm 0.08 \pm 0.03.$$

Using the value of the  $\Lambda_c^+ \rightarrow \Xi(1690)^0 K^+$ ,  $\Xi(1690)^0 \rightarrow \Sigma^+ K^-$  combined branching ratio, obtained in Section 5, and the ratio of the normalization decay rates [2], we find the following ratio of  $\Xi(1690)^0$  decay rates:

$$\frac{\mathcal{B}(\Xi(1690)^0 \rightarrow \Sigma^+ K^-)}{\mathcal{B}(\Xi(1690)^0 \rightarrow \Lambda^0 \bar{K}^0)} = 0.50 \pm 0.26.$$

The corresponding ratio of the  $\Xi(1690)^0$  decay rates quoted by [2] ( $1.8 \pm 0.6$  after isospin correction) is based on a single measurement reported in [6]. In order to check for possible interference

ture above a smooth background. We have also searched for the  $\Lambda_c^+ \rightarrow \Xi(1690)^0 K^+$  decay in the  $\Lambda_c^+ \rightarrow (\Xi^- \pi^+) K^+$  decay mode, but did not find any  $\Xi(1690)^0$  signal in the  $\Xi^- \pi^+$  invariant mass spectrum, in agreement with the  $\mathcal{B}(\Xi(1690)^0 \rightarrow \Xi^- \pi^+)$  upper limit value from [6].

## 7 Measurement of the $\Lambda_c^+ \rightarrow pK^+K^-$ and $\Lambda_c^+ \rightarrow p\phi$ decays

The first evidence for the  $\Lambda_c^+ \rightarrow p\phi$  decay was reported by NA32 in 1990, who claimed a signal of  $2.8 \pm 1.9$  events [7]. The decay  $\Lambda_c^+ \rightarrow pK^+K^-$  was observed for the first time by E687 in 1993, who also obtained an upper limit for the branching ratio of  $\Lambda_c^+ \rightarrow p\phi$  [8]. The most recent statistically significant resonant analysis was published by CLEO in 1996, who found the following branching ratios:  $\mathcal{B}(\Lambda_c^+ \rightarrow pK^+K^-)/\mathcal{B}(\Lambda_c^+ \rightarrow pK^- \pi^+) = 0.039 \pm 0.009 \pm 0.007$  and  $\mathcal{B}(\Lambda_c^+ \rightarrow p\phi)/\mathcal{B}(\Lambda_c^+ \rightarrow pK^- \pi^+) = 0.024 \pm 0.006 \pm 0.003$  [9].

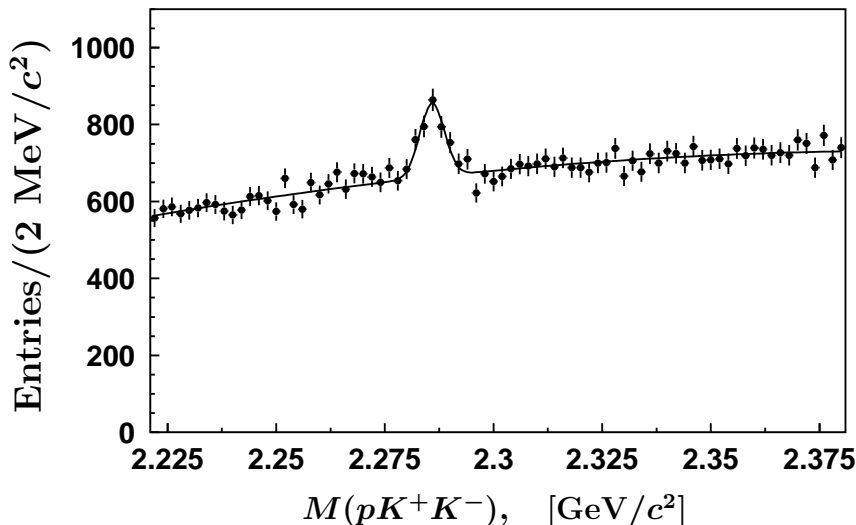


Figure 8:  $\Lambda_c^+ \rightarrow pK^+K^-$ : invariant mass spectrum of the selected  $pK^+K^-$  combinations.

Reconstructing  $\Lambda_c^+ \rightarrow pK^+K^-$  candidates according to the procedure described in Section 2, we see a clear peak at the  $\Lambda_c^+$  mass, as shown in Fig. 8. We fit the distribution with a Gaussian (with width fixed to  $2.8 \text{ MeV}/c^2$  from the MC) plus a second order polynomial, and find  $676 \pm 89$   $\Lambda_c^+ \rightarrow pK^+K^-$  events. For normalization we reconstruct the  $\Lambda_c^+ \rightarrow pK^- \pi^+$  decay mode with equivalent cuts and fit the distribution with a double Gaussian for the large signal peak, and a second order polynomial, finding  $51680 \pm 650$  events. The relative efficiency of the  $\Lambda_c^+ \rightarrow pK^-K^+$  decay reconstruction with respect to  $\Lambda_c^+ \rightarrow pK^- \pi^+$  is found to be 0.93 in the MC: using this value, we extract

$$\frac{\mathcal{B}(\Lambda_c^+ \rightarrow pK^+K^-)}{\mathcal{B}(\Lambda_c^+ \rightarrow pK^- \pi^+)} = 0.014 \pm 0.002 \pm 0.002.$$

In order to obtain the  $\Lambda_c^+ \rightarrow p\phi$  signal we take  $pK^+K^-$  from a  $\pm 6 \text{ MeV}/c^2$  window around the fitted  $\Lambda_c^+$  mass ( $2286 \text{ MeV}/c^2$ ), and plot the invariant mass of the  $K^+K^-$  combination, as shown in

sideband intervals centered  $13 \text{ MeV}/c^2$  below and above the fitted  $\Lambda_c^+$  mass (shaded histogram). The

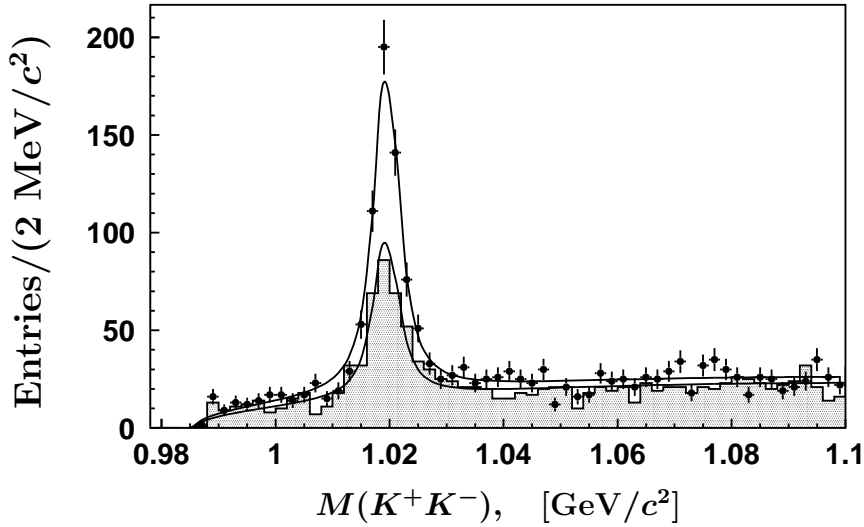


Figure 9: Fitting for the  $\Lambda_c^+ \rightarrow p\phi$  component: the invariant mass spectra of  $K^+K^-$  combinations from the  $\Lambda_c^+ \rightarrow pK^+K^-$  signal area (points with error bars) and sidebands (shaded histogram).

distributions are fitted using a method similar to that used for the  $\Lambda_c^+ \rightarrow \Sigma^+\phi$  analysis (Section 5). After making a sideband subtraction and correction for the signal outside the  $\Lambda_c^+$  mass interval we obtain  $345 \pm 43 \Lambda_c^+ \rightarrow p\phi$  decays.

The reconstruction efficiency of the  $\Lambda_c^+ \rightarrow p\phi$  decay relative to  $\Lambda_c^+ \rightarrow pK^-\pi^+$  was calculated using the MC and found to be 0.89. Using this value, we extract

$$\frac{\mathcal{B}(\Lambda_c^+ \rightarrow p\phi)}{\mathcal{B}(\Lambda_c^+ \rightarrow pK^-\pi^+)} = 0.015 \pm 0.002 \pm 0.002.$$

The non- $\phi$   $\Lambda_c^+ \rightarrow pK^+K^-$  signal is estimated by making an invariant mass cut  $|M(K^+K^-) - m_\phi| > 10 \text{ MeV}/c^2$  to suppress the  $\phi \rightarrow K^+K^-$  contribution. After fitting the resulting  $pK^+K^-$  mass spectrum and applying corrections accounting for the  $\phi$  tails and the missing phase space region around the  $\phi$  mass we obtain  $344 \pm 81 \Lambda_c^+ \rightarrow pK^+K^-$  non- $\phi$  decays. This corresponds to

$$\frac{\mathcal{B}(\Lambda_c^+ \rightarrow pK^+K^-)_{\text{non-}\phi}}{\mathcal{B}(\Lambda_c^+ \rightarrow pK^-\pi^+)} = 0.007 \pm 0.002 \pm 0.002.$$

## 8 Systematic errors

We have considered several possible sources for the systematic errors in our measurements. The most important is the uncertainty in the pion and kaon identification efficiencies, which affects all ratios of signal and reference branchings. Based on a study of kaons and pions from  $D^{*+}$ -tagged  $D^0 \rightarrow K^-\pi^+$  decays, we assign a systematic uncertainty of 6% per  $K/\pi$  ratio (*e.g.* 6% for  $\Lambda^0 K^+/\Lambda^0 \pi^+$ , 12% for  $\Sigma^+ K^+K^-/\Sigma^+ \pi^+\pi^-$ ).

background function has been varied by changing the order of the polynomial function, with any change in the signal yield being taken as a systematic uncertainty. For each fit where the width of the signal Gaussian was fixed to the MC prediction, we have redone the fit with a floating width, and taken the resulting change in the yield as a systematic uncertainty. For the  $\Lambda_c^+ \rightarrow pK^+K^-$  and  $\Lambda^0K^+$  analyses, we have assigned additional uncertainties of 6% and 10% respectively on the signal yields, based on the fractions of signal events found in non-Gaussian tails for the normalization modes  $pK^-\pi^+$  and  $\Lambda^0\pi^+$  (the  $pK^+K^-$  and  $\Lambda^0K^+$  samples are too small to fit for the presence of non-Gaussian tails).

For the Breit-Wigner fit of the  $\phi$  signal we have varied the function by letting the width of the convolved Gaussian float and varying the shape of the background parameterization. We have also included the 1.4% uncertainty of  $\mathcal{B}(\phi \rightarrow K^+K^-)$  and varied the  $\phi$  nominal width within its error [2]. In the case of  $\Lambda_c^+ \rightarrow \Sigma^+\phi$  and  $p\phi$  decays there is an additional source of systematic error due to the difference in kinematics between the signal and normalization modes. This has been estimated to be 6% for  $\Sigma^+\phi$  and 4% for  $p\phi$ , based on the difference between the MC predictions for the efficiency in resonant and non-resonant cases.

In the  $\Lambda_c^+ \rightarrow \Xi(1690)^0K^+$ ,  $\Xi(1690)^0 \rightarrow \Sigma^+K^-$  resonant analysis we neglected the possible interference between  $\Xi(1690)^0$  and  $\phi$  contributions. MC studies show that this leads to an uncertainty of less than 5%, due to phase space limitations in the interference region.

## 9 Conclusions

In summary, we report the first observation of the Cabibbo-suppressed decays  $\Lambda_c^+ \rightarrow \Lambda^0K^+$  and  $\Lambda_c^+ \rightarrow \Sigma^0K^+$ , and the first observation of  $\Lambda_c^+ \rightarrow \Sigma^+K^+\pi^-$  with large statistics. The decays  $\Lambda_c^+ \rightarrow pK^+K^-$ ,  $\Lambda_c^+ \rightarrow p\phi$  and  $\Lambda_c^+ \rightarrow (pK^+K^-)_{\text{non-}\phi}$ , and the W-exchange decays  $\Lambda_c^+ \rightarrow \Sigma^+K^+K^-$  and  $\Lambda_c^+ \rightarrow \Sigma^+\phi$  have been measured with the best accuracy to date. We have also observed evidence for the decay  $\Lambda_c^+ \rightarrow \Xi(1690)^0K^+$  and set an upper limit on the non-resonant decay mode  $\Lambda_c^+ \rightarrow \Sigma^+K^+K^-$ . The results for these decay modes are listed in Table 1.

## 10 Acknowledgment

We wish to thank the KEKB accelerator group for the excellent operation of the KEKB accelerator. We acknowledge support from the Ministry of Education, Culture, Sports, Science, and Technology of Japan and the Japan Society for the Promotion of Science; the Australian Research Council and the Australian Department of Industry, Science and Resources; the Department of Science and Technology of India; the BK21 program of the Ministry of Education of Korea and the CHEP SRC program of the Korea Science and Engineering Foundation; the Polish State Committee for Scientific Research under contract No.2P03B 17017; the Ministry of Science and Technology of Russian Federation; the National Science Council and the Ministry of Education of Taiwan; and the U.S.

# References

- [1] Y. Kohara, *Nuovo Cim.* **A** 111 (1998) 67;  
M. A. Ivanov et al., *Phys. Rev.* **D** 57 (1998) 5632;  
K. K. Sharma and R. C. Verma, *Phys. Rev.* **D** 55 (1997) 7067;  
L. Chau et al., *Phys. Rev.* **D** 54 (1996) 2132;  
A. Datta, hep-ph/9504428;  
T. Uppal et al., *Phys. Rev.* **D** 49 (1994) 3417;  
P. Zenczykowski, *Phys. Rev.* **D** 50 (1994) 402;  
J. Körner and M. Krämer, *Z. Phys.* **C** 55 (1992) 659.
- [2] D. E. Groom et al., *EPJ* **C** 15 (2000) 1 and 2001 off-year partial update
- [3] A. Abashian et al. (Belle Collaboration), KEK Progress Report 2000–4 (2000),  
to be published in *Nucl. Instr. Meth.* **A**.
- [4] S. Barlag et al. (NA32 Collaboration), *Phys. Lett.* **B** 283 (1992) 465.
- [5] P. Avery et al. (CLEO Collaboration), *Phys. Rev. Lett.* 71 (1993) 2391.
- [6] C. Dionisi et al., *Phys. Lett.* **B** 80 (1978) 145.
- [7] S. Barlag et al. (NA32 Collaboration), *Z. Phys.* **C** 48 (1990) 29.
- [8] P. L. Frabetti et al. (E687 Collaboration), *Phys. Lett.* **B** 314 (1993) 477.
- [9] J. P. Alexander et al. (CLEO Collaboration), *Phys. Rev.* **D** 53 (1996) R1013.
- [10] Y. Kubota et al. (CLEO Collaboration), *Phys. Rev. Lett.* 71 (1993) 3255.



Table 1. Summary of the results obtained in this paper.

The last column shows the most accurate previous measurement of each decay mode, where applicable.

$\Lambda_c^+$ signal mode	Signal yield	$\Lambda_c^+$ reference mode	Reference yield	Relative efficiency	$\mathcal{B}_{\text{signal}}/\mathcal{B}_{\text{reference}}$	Other measurements
$\Lambda^0 K^+$	$265 \pm 35$	$\Lambda^0 \pi^+$	$4550 \pm 111$	0.79	$0.074 \pm 0.010 \pm 0.012$	—
$\Sigma^0 K^+$	$75 \pm 18$	$\Sigma^0 \pi^+$	$1597 \pm 67$	0.84	$0.056 \pm 0.014 \pm 0.008$	—
$\Sigma^+ K^+ \pi^-$	$105 \pm 24$	$\Sigma^+ \pi^+ \pi^-$	$2368 \pm 89$	0.94	$0.047 \pm 0.011 \pm 0.008$	$0.24_{-0.16}^{+0.24}$ [4]
$\Sigma^+ K^+ K^-$	$246 \pm 20$	$\Sigma^+ \pi^+ \pi^-$	$3650 \pm 138$	0.89	$0.076 \pm 0.007 \pm 0.009$	$0.094 \pm 0.017 \pm 0.019$ [5, 10]
$\Sigma^+ \phi$	$129 \pm 17$	$\Sigma^+ \pi^+ \pi^-$	$3650 \pm 138$	0.84	$0.085 \pm 0.012 \pm 0.012$	$0.094 \pm 0.033 \pm 0.025$ [5, 10]
$\Xi(1690)^0 K^+, \Xi(1690)^0 \rightarrow \Sigma^+ K^-$	$75 \pm 16$	$\Sigma^+ \pi^+ \pi^-$	$3650 \pm 138$	0.89	$0.023 \pm 0.005 \pm 0.005$	—
$\Xi(1690)^0 K^+, \Xi(1690)^0 \rightarrow \Lambda^0 \bar{K}^0$	$93 \pm 26$	$\Lambda^0 \bar{K}^0 K^+$	$363 \pm 26$	1.00	$0.26 \pm 0.08 \pm 0.03$	—
$\Sigma^+ K^+ K^-$ (non-res)	—	$\Sigma^+ \pi^+ \pi^-$	$3650 \pm 138$	0.89	$< 0.018$ @ 90% CL	—
$pK^+ K^-$	$676 \pm 89$	$pK^- \pi^+$	$51680 \pm 650$	0.93	$0.014 \pm 0.002 \pm 0.002$	$0.039 \pm 0.009 \pm 0.007$ [9]
$p\phi$	$345 \pm 43$	$pK^- \pi^+$	$51680 \pm 650$	0.89	$0.015 \pm 0.002 \pm 0.002$	$0.024 \pm 0.006 \pm 0.003$ [9]
$pK^+ K^-$ (non- $\phi$ )	$344 \pm 81$	$pK^- \pi^+$	$51680 \pm 650$	0.93	$0.007 \pm 0.002 \pm 0.002$	—